Geomechanics and Engineering, *Vol. 36, No. 4 (2024) 391-406*
https://doi.org/10.12989/gae.2024.36.4.391

Experimental research on dynamic characteristics of frozen clay considering seasonal variation

Xuyang Bian[1,2], Guoxin Wang*[1,2] and Yuandong Li[3b]

[1]*State Key Laboratory of Coastal and Offshore Engineering, Dalian University of Technology, Dalian, Liaoning, 116024, China*
[2]*Institute of Earthquake Engineering, Faculty of Infrastructure Engineering, Dalian University of Technology, Dalian, Liaoning, 116024, China*
[3]*School of Transportation Engineering, Nanjing Tech University, Nanjing, China*

(*Received October 23, 2023, Revised January 23, 2024, Accepted January 26, 2024*)

Abstract. In order to study the soil seasonal dynamic characteristics in the regions with four distinct seasons, the soil dynamic triaxial experiments were conducted by considering the environmental temperature range from -30°C to 30°C. The results demonstrate that the dynamic soil properties in four seasons can change greatly. Firstly, the dynamic triaxial experiments were performed to obtain the dynamic stress-strain curve, elastic modulus, and damping ratio of soil, under different confining pressures and temperatures. Then, the experiments also obtain the dynamic cohesion and internal friction angle of the clay under the initial strain, and the changing rule was summarized. Finally, the results show that the dynamic elastic modulus and dynamic cohesion will increase significantly when the clay is frozen; as the temperature continues to decrease, this increasing trend will gradually slow down, and the dynamic damping ratio will go down when the freezing temperature decreases. In this paper, the change mechanism is objectively analyzed, which verifies the reliability of the conclusions obtained from the experiment.

Keywords: dynamic cohesion; dynamic damping ratio; dynamic elastic modulus; dynamic triaxial tests; seasonal frozen clay

1. Introduction

In China, seasonally frozen soil occupies 53.5% of China's total land area (Zheng *et al.* 2002), as shown in Fig. 1. When winter comes, the surface layer soil in these areas will freeze for about half a year. When winter passes and summer comes, the surface soil will gradually melt, so this layer of soil is called the freeze-thaw layer. Such a freezing and thawing phenomenon is repeated continuously with the environmental temperature changing, which affects dynamic soil properties directly and obviously, leading to hidden dangers to the stability and safety of surrounding engineering structures.

Dynamic soil properties can be influenced by many factors, including region, temperature, geological conditions, soil age, etc. The difference of these factors will cause great differences in the dynamic soil properties (Wang *et al*. 2017). Fredlund (2006) extensively researched the mechanics of unsaturated soils, laying the foundation for understanding the characteristics of unsaturated soil mechanics. Thomas *et al.* (2010) studied the drying effects on unsaturated cohesive soil, emphasizing the necessity of investigating variations in soil moisture levels with changing seasons. Zhang (2012) provided a comprehensive

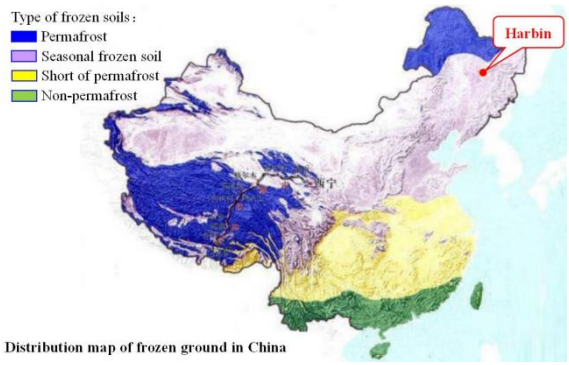

Fig. 1 Seasonal frozen soil area of China

analysis of the research progress on the dynamic characteristics of sand, suggesting that the analysis of soil dynamic characteristics should be based on constitutive relationships while considering the changing patterns of soil dynamics under factors like high temperatures and cold conditions. Currently, numerous experiments are being conducted to study soil characteristics, encompassing conventional triaxial tests, dynamic triaxial tests, and low-temperature triaxial tests. Kang *et al.* (2015) conducted strain-controlled cyclic simple shear tests on silica sand using the radial strain measurement method. They found that the higher the confining pressure, the smaller the volume change. When the confining pressure exceeded 200 kPa, the volume change was less than 0.1%. Additionally, Kang *et al*. (2015) proposed that the improved cyclic simple shear test could better replicate field conditions. Le *et al.*

*Corresponding author, Professor
E-mail: gxwang@dlut.edu.cn
[a]Ph.D. Student
[b]Ph.D. Student

ISSN: 2005-307X (Print), 2092-6219 (Online)

(2017) researched the dynamic properties of unsaturated sand using a custom-made direct simple shear testing device. They demonstrated that this device could continuously capture changes in the dynamic properties of unsaturated sand. Cheng *et al.* (2021) used freeze-thaw cycle tests and consolidated drained triaxial tests, finding that saline soil exhibited strain hardening in its stress-strain relationship. Chen *et al*. (2017) developed a triaxial testing apparatus that can be used in conjunction with medical CT scanners, enabling high-quality imaging of the microstructural changes in soil. Different regions and soil types exhibit diverse dynamic properties, with notable distinctions observed between soil at normal temperature and frozen soil. Regarding different soil types at normal temperatures, Voottipruex *et al*. (2014) conducted research on the expansive soil in northern Thailand and found that different soil types affect the soil's expansion pressure. Mosallamy *et al*. (2016) conducted resonance column tests on Egyptian loess, concluding that an elevation in confining pressure leads to a reduction in the damping ratio. Reznik *et al.* (2007) studied the physical properties of collapsible loess and discovered that its collapsibility induces significant changes in its physical characteristics. Garakani *et al*. (2015) investigated collapsible loess through indoor dynamic triaxial tests, revealing that the cohesion of the loess decreases with increased moisture content, while the internal friction angle increases with higher moisture content. Kallioglou *et al*. (2008) employed a resonance column apparatus to test the small-strain dynamic shear modulus and damping ratio of Greek clay, thereby establishing the attenuation curve of the dynamic shear modulus. Mu *et al.* (2020) conducted tests on the dynamic properties of undisturbed red clay in Guiyang, China, and they proposed the concept of equivalent dynamic elastic modulus, and obtained the dynamic elastic modulus of undisturbed red clay under different confining pressures and vibration times. Onur *et al.* (2014) discovered, through experiments, a continuous increase in the shear modulus of sand with rising saturation. Güler *et al*. (2021) conducted dynamic triaxial and resonant column tests on cohesive sand in Turkey, determining the patterns of stress-strain curves and concluding that the damping ratio undergoes significant changes with varying lateral pressure. Yasuhara *et al.* (2003) conducted an undrained dynamic triaxial test on the soil, and the results demonstrated that vibration times had a strong impact on the dynamic soil properties. Teachavorasinskun *et al*. (2002) researched soft soil in the Bangkok area using indoor dynamic triaxial and resonant column tests, concluding that consolidation time has the greatest impact on the dynamic shear modulus and damping ratio of soft soil. Shogaki *et al*. (2003) extensively researched soft soil in the Busan region of South Korea through numerous indoor experiments, studying detailed patterns of changes in its microstructure, and physical and mechanical properties, among other parameters. Tamotsu *et al.* (2004) studied borehole data of thick-layered soft soil in the Osaka Bay area of Japan, deriving the physical characteristics of the soft soil in that region. Abuel-Naga *et al*. (2009) performed indoor tests on soft soil in the Bangkok area, finding that the thermal conductivity of soft soil increases with the density of the soil mass. Okamura *et al.* (2011) conducted experimental research on soft soil foundations using a centrifuge, revealing that during vibration, there is a significant increase in pore water pressure within the soft soil. Yang *et al.* (2018) used GCTS dynamic hollow cylindrical torsional shear apparatus to conduct dynamic cyclic tests on Tianjin Binhai marine soft soil and found that under cyclic loading, the damping ratio evolution and dynamic compression modulus of the soil were related to the amplitude of the applied load. It was concluded that at low amplitude, the shear strength of the soil would decrease with the increase of the number of vibrations and gradually stabilize.

In terms of frozen soil research. Li *et al.* (2017) elaborated on the main factors affecting the properties of frozen soil, including soil quality, moisture content and confining pressure. Wijeweera *et al.* (1990, 1991, 2011) examined the influence of moisture content, and soil type on the compressive strength of frozen soil and put forward empirical formulas for predicting the compressive strength of frozen soil. Christ *et al*. (2009) analyzed the dynamic elastic modulus and damping ratio of frozen soil under different confining pressures and water content. Girgis *et al.* (2019, 2020) conducted uniaxial compression tests on frozen sandy clay, establishing a linear relationship between Young's modulus of frozen clay and temperature within the range of -15°C to 0°C. Esmaeili-Falak *et al*. (2019, 2020) concluded, through triaxial compression tests, that non-cohesive soil transitions from a hardening-type stress-strain curve to a softening-type curve after freezing. Tounsi *et al.* (2020) conducted triaxial compression tests on frozen metamorphic shale, determining that the stress-strain curve of frozen metamorphic shale is highly sensitive to changes in temperature and confining pressure. Kim *et al*. (2021) studied the effects of ice content and fine content on frozen sand-silt mixtures through unconfined compression tests, concluding that the unconfined compressive strength increases with higher ice content and pore ratio. Yamamoto *et al.* (2014) conducted triaxial constant strain rate tests and constant stress creep tests on artificial frozen soil samples, discovering that ice content does not affect shear strength when the ice volume exceeds 40%. Ma *et al*. (2021) elaborated on the research progress of the seismic response of permafrost sites in the Qinghai Tibet region and mentioned that studying the dynamic characteristics of permafrost sites should be combined with actual engineering geological conditions to make the research results closer to the actual site situation. Shelman *et al.* (2014) studied the dynamic elastic modulus changes of five typical soils at different freezing temperatures. Czajkowski *et al.* (1980) concluded through experiments that the dynamic elastic modulus of soil increases upon freezing. Similarly, Wu *et al*. (2019), Xu *et al*. (2020) also found that the dynamic elastic modulus increases with soil freezing. Li *et al.* (2016) mentioned that when soil undergoes freezing, its strength can increase by a factor of 10 to 20. It is concluded that the elastic modulus of the soil increases by 300 times after freezing. Fard *et al*. (2020) highlighted the significant impact of freeze-thaw cycles on the engineering properties of frozen soil. Viran *et al.* (2018) investigated the

Table 1 Temperature change in Harbin

Month	Daily average maximum temperature(°C)	Daily average minimum temperature(°C)	Historical maximum temperature(°C)	Historical minimum temperature(°C)
January	-14	-25	-1	-34
February	-8	-20	6	-30
March	3	-9	22	-24
April	15	2	32	-7
May	22	11	34	1
June	28	17	38	9
July	29	20	35	14
August	27	19	35	8
September	22	11	29	-2
October	12	1	25	-12
November	0	-9	16	-24
December	-11	-21	7	-32

changes in the physical and mechanical properties of clay before and after freeze-thaw cycles, observing a reduction of 38.54% in cohesion and 36.99% in the internal friction angle of the clay after freeze-thaw cycles. Aldaood *et al*. (2016) conducted experimental research on lime-treated gypsum soil, concluding that moisture and gypsum content significantly affect the properties of the soil after freeze-thaw cycles. Kumar *et al*. (2020) studied the physical properties of plastic soil after freezing and thawing, noting a 128.97% increase in unconfined compressive strength after three freeze-thaw cycles. Lee *et al.* (2020) performed uniaxial compression tests on sand-silt mixtures, determining that the unconfined compressive strength decreases with an increase in the volume of unfrozen water and the number of repeated load applications.

It can be seen from the above contents that there is much research on soil dynamic parameters at present, and the soil dynamic test technology is also relatively mature. However, there is still a lack of systematic research on the evolution laws of soil dynamic properties considering seasonal variations. Because of the huge area of seasonally frozen soil in the world, season change has a significant impact on the soil, and the change of soil parameters will have a great impact on the ground structure, which endows this research with great necessity. Based on previous studies, this paper considers the impact of seasonal changes on clay dynamics, sets different temperatures to simulate seasonal changes in the test process, and quantitatively analyzes their differences. In previous experimental studies, the majority of tests involved removing the soil sample from the freezer after it reached the freezing temperature and then installing it in the triaxial test box for testing. During the process of sample removal and installation, the temperature tends to increase, resulting in errors in the test results. However, in the experiment described in this article, the triaxial tester is directly connected to the temperature control box. To better simulate the environmental temperature, the triaxial tester can be set to a specific temperature to ensure that the test box reaches the desired temperature. Throughout the entire experiment, there is no temperature loss, effectively avoiding errors in the test results.

This paper not only obtained the results of the dynamic elastic modulus and dynamic damping ratio, but also studied the dynamic internal friction angle and dynamic cohesion of the clay, and considered the impact of different freezing temperatures on the dynamic parameters of the soil sampled in Harbin as shown in Fig. 1 where is very cold in almost half year winter season as surveyed throughout the year in Table 1, it can be seen that the historical minimum temperature in Harbin is -34°C and maximum temperature is 38°C; the daily average minimum temperature is about -25°C and the daily average maximum temperature is about 29°C. According to the findings from the investigation, in seasonal frozen soil regions, during winter, temperatures mostly fall below -20°C. In summer, temperatures are consistently positive. During spring and autumn, temperatures generally range between positive temperatures and -15°C. The experiment studied the dynamic parameters of clay under different temperatures and different confining pressures. The temperature is set based on the results of the investigation, which is the normal temperature (23°C), -5°C, -10°C, -15°C and -20°C. The positive temperature was set at 23°C, as preliminary surveys indicated that summer temperatures were mostly above 20°C. Within the range of positive temperatures attainable in summer, fluctuations in temperature have a negligible impact on soil property parameters. Since the experiments were conducted in winter, to better simulate summer temperatures, the indoor temperature at the time was set to the required positive temperature for the experiments, which was 23°C. To better observe the variability, the interval of 5°C is used for the setting of negative temperature, and it provides a better simulation of the transitions between seasons. To better analyze the evolving patterns of soil dynamic properties with seasonal variations, this study sets the temperature for summer at 23°C. The temperature is set to -5°C for late spring and early autumn. For early spring and late autumn, the temperatures are set at -10°C and -15°C. The temperature for winter is set at -20°C.

2. Dynamic triaxial test

2.1 Test equipment

UTM-100 in the lab of Heilongjiang Institute of

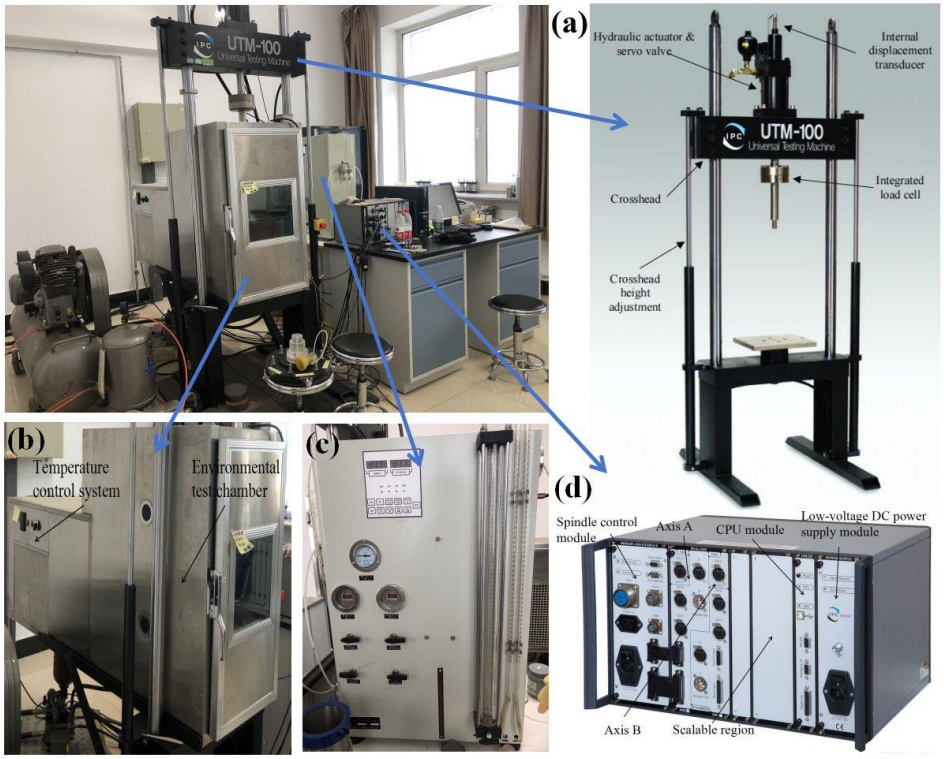

Fig. 2 UTM-100 universal testing machine: (a) UTM-100 loading frame, (b) Environmental chamber, (c) Confining pressure loading instrument and (d) IMACS

Technology, Harbin, China is used as the instrument used for triaxial test. This instrument has high accuracy and stability. The rheological properties of the material are measured by tension, compression, and dynamic loading. It is suitable for various materials, like asphalt mixture, concrete, soil, unbound granular materials, fibers and plastics, etc. The test equipment consists of an electro-hydraulic loading system, a confining pressure system, an environmental chamber, and a corresponding control system. It has a highly improved geotechnical triaxial chamber, which also serves as an environmental chamber and uses air as a confining pressure medium. The electric power requirement of the environmental box is 115 V/60 Hz 25 A or 240 V/50 Hz 15 A. The test control is based on a computer, and the feedback signal is obtained by the sensor on the device, and the additional sensor is used for virtual feedback. At the same time, the triaxial testing machine is directly connected to the temperature control box, which ensures that the test process is carried out at the required temperature, to make it closer to the real external environment, as shown in Fig. 2.

Fig. 2(a) shows the UTM-100 loading frame, consisting of a crossbeam and a base. It is connected by two chrome-plated columns to form a basic reaction loading frame. The position of the upper crossbeam can be adjusted using two auxiliary hydraulic lifting pistons. The range of static loading is 130 kN. The range of fatigue loading is 100 kN.

The actuator stroke is 100 mm. The maximum speed of the actuator is 1200 mm/min. The pressure sensor is ±100 kN (the accuracy is 0.1%). Fig. 2(b) shows the environmental chamber, with the latter half dedicated to the temperature control system, which achieves a temperature adjustment accuracy of 0.1°C. Fig. 2(c) represents the confining pressure loading instrument, where pneumatic pressure is used for loading in this test. Fig. 2(d) represents an integrated multi-axis control system (IMACS) with a closed-loop sampling rate of up to 2.5 kHz. It offers three feedback control modes: force, position, and strain. The displacement sensor has a range of 100mm, the force sensor has a range of ±100 kN, and the confining pressure sensor has a range of ±1000 kPa.

2.2 Test soil

The soil in the test was clay in Harbin. Because the test was carried out in winter, the average temperature in Harbin had reached about -20°C during the test, and the surface soil had been frozen firmly. The clay used in the test was collected from a construction site, the depth of the soil was about 2.5 m below the surface. The depth for soil extraction is determined based on actual field surveys. Before the extraction, a preliminary study was conducted on the frozen soil layer depths across various regions in Heilongjiang Province. It was found that the thickness of the frozen soil layers in most cities ranged between 1.8 to 2.6 m. Taking into account the ambient environmental temperatures at that time, the depth for soil extraction was thus set at 2.5 m. As the construction site was in a semi-suspended state, the soil within was not firmly frozen and was marked by the presence of a foundation pit. During soil extraction, we utilized an excavator in conjunction with manual digging to collect the soil samples at specific depths. The collected soil

Fig. 3 Clay in Harbin

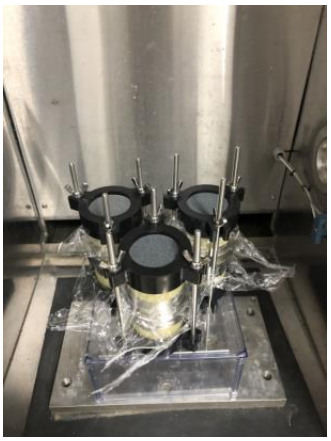

Fig. 4 Soil sample

was then transported to the laboratory. The test soil sample was a cylindrical soil sample with a diameter of 50 mm and a height of 100 mm. To achieve a uniform distribution of soil samples, a layered compaction method is employed during the manufacturing process. In order to lower the test error, three groups of soil samples with close test results were taken under each working condition, and then the average value was taken as the test result. In order to better compare the soil dynamic properties at the normal temperature and various freezing temperatures, the moisture content of the soil sample was set more strictly. In order to get a more suitable moisture content, the test process was carried out for the clay with various moisture content. In the preliminary test, the moisture content was 5%, 10%, 15%, 20%, and 25%. According to the soil sample preparation and the deformation of the soil sample during the test, when the moisture content was 5%, the freezing effect and the freezing temperature had little effect on it. When the moisture content was set to 25%, due to the high moisture content, the normal temperature soil sample would be greatly deformed during the production process and the sample installation process, leading to inaccurate test results. According to the problems of pre-test clay samples, at the same time, in order to better compare the difference between non-frozen soil and frozen soil at various temperatures, the clay moisture content was finally determined at 15%.

In order to prepare the moisture content of the clay, firstly, the clay soil sample was naturally dried massively at normal temperature and then vibrated the dried soil. After vibrating, pass through a sieve with a diameter of 2 mm, and then put the vibrated soil in the oven to dry it further and completely remove the remaining moisture in the soil. Fig. 3 shows the soil specimen after drying.

Then weigh a certain quality of soil into the test basin, and weigh the water of the corresponding quality, spray it into the test basin in batches, stir evenly, and finally seal the test basin with plastic wrap to prevent the loss of water. Let it stand still for more than 24 hours to make the water fully combined with clay, and then make the test soil sample. In the preparation of soil samples, we initially prepared molds with an inner diameter of 50mm and a height of 100 mm.

The inside of the mold was coated with Vaseline to facilitate the extraction of the prepared soil sample. Subsequently, clay was placed into the mold and compacted in layers, with each layer undergoing a scraping process to ensure the continuity and integrity of the soil sample. A forming tube was then prepared, with a latex membrane inverted over it, and the air between the forming tube and the latex membrane was extracted. Finally, the soil sample in the mold was placed into the forming tube. The soil sample was fixed with a holder and frozen at a constant temperature. The freezing process was conducted directly in an environmental chamber, as shown in Fig. 2(b), utilizing a temperature control system to adjust to the required temperature. The soil samples are covered at both ends with cling film and impermeable stones to prevent moisture loss, as shown in Fig. 4. The confining pressures set in the test were 100 kPa, 20 0kPa, and 300 kPa, and the consolidation ratio was 1. Fig. 5 shows the sample loading process. Firstly, the soil samples are installed in the pressure chamber outdoors, and then the bolts of the pressure chamber are tightened to ensure a completely sealed state. Next, the pressure chamber is installed in the environmental chamber, and the chamber door is immediately closed. After a period of rest, when the temperature inside the environmental chamber reaches the desired level, confining pressure is applied. The application of confining pressure was carried out using the confining pressure loading device shown in Fig. 2(c). From Fig. 5(c), it can be observed that the soil samples are tightly wrapped without any signs of loosening. This indicates that the confining pressure was successfully applied. Finally, the experiment begins.

2.3 Loading method

The test adopted a cyclic loading method with a frequency of 1 Hz and a step-by-step loading method. The loading was divided into 10 levels; each level was 1 minute in duration; each level was divided into 6 stages; each stage had a duration of 10 seconds. For normal temperature soil, the loading force of each stage was set to 5 kN; for frozen soil, the loading force of each stage was set to 50 kN. Control of the IMACS was conducted via computer. IMACS is the core control component of UTM-100, and it was used to ensure the stable operation of the loading frame, thereby ensuring the smooth progress of the experiment. For dynamic triaxial tests, the main observed strain was between 10-4 and 10-2 (Bo *et al*. 2021). Fig. 6

(a) (b) (c) (d)

Fig. 5 Test process

(a) (b) (c)

Fig. 6 Change of soil sample and profile

shows the comparison diagram of the clay sample before and after the test, and the cross-sectional view of the sample. Fig. 6(a) shows that before the experiment, the soil sample was in a regular cylindrical shape. After the experiment, the soil sample was subjected to forces and exhibited bulging, as shown in Fig. 6(b). Fig. 6(c) presents the cross-sectional view after cutting the soil sample with a cutter.

3. Dynamic parameters

3.1 Dynamic elastic modulus

The dynamic elastic modulus is an important dynamic parameter that reflects the dynamic stress-strain relationship of the soil in the elastic phase. Due to the certain viscosity of the clay in different states, the dynamic stress-strain hysteresis loop obtained by the test results shows that the maximum dynamic stress and the maximum dynamic strain do not correspond to each other. Fig. 7 shows the dynamic stress-strain curve relationship in the test.

The dynamic modulus of elasticity adopts secant modulus (Ishihara *et al*. 1985), which can be calculated by the following Eq. (1)

$$E_d = \frac{\sigma_d - \sigma_0}{\varepsilon_d - \varepsilon_0} \tag{1}$$

where σ_d is the maximum dynamic stress, σ_0 is the minimum dynamic stress, ε_d is the maximum dynamic strain, and ε_0 is the minimum dynamic strain.

3.2 Dynamic damping ratio

The dynamic damping ratio is an important index reflecting the vibration energy absorbed by the soil, and it is an indispensable parameter in analyzing the dynamic response of frozen soil. The dynamic damping ratio is the ratio of the area of the hysteresis loop to the area of the triangle enclosed by it, as shown in Fig. 8. It is the ratio of the elastic strain energy in a cyclic period to the energy lost in the cyclic period, where $S_{ellipse}$ represents the area of the hysteresis loop, and $S_{\square ABC}$ represents the area of the triangle, and it is calculated using the following Eq. (2) (Xie 2011).

$$\lambda = \frac{S_{ellipse}}{\pi S_{\triangle ABC}} \tag{2}$$

When the area of the hysteresis loop and triangle is small, the dynamic damping is relatively small. At the same time, the shape of the hysteresis loop can also represent the size of the dynamic damping ratio. When the shape of the hysteresis loop is rounder, the damping is relatively larger, and vice versa.

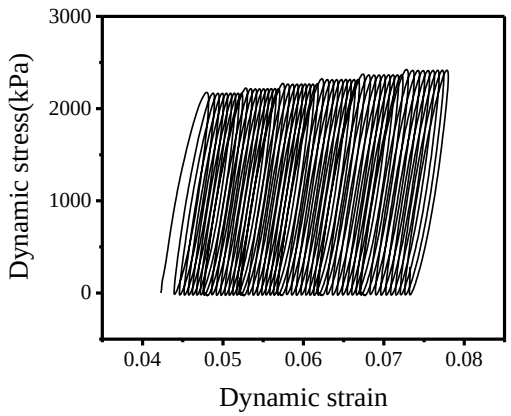

Fig. 7 Dynamic stress-strain curve

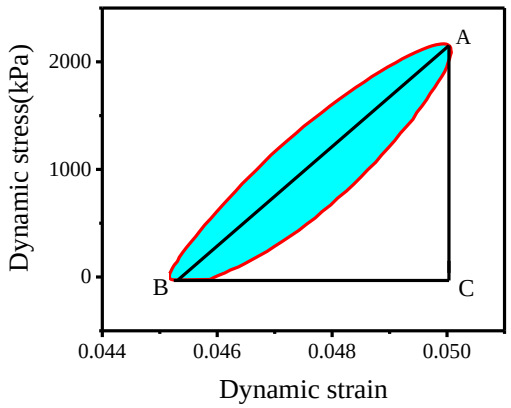

Fig. 8 Dynamic stress-strain hysteresis loop

3.3 Dynamic cohesion and dynamic internal friction angle

Dynamic cohesion c reflects various physical and chemical forces between soil particles under cyclic loading, including Van der Waals force, cementing force, Coulomb force, etc., mainly determined by the cementing force of the cementing material and the distance between particles. The dynamic internal friction angle φ mainly shows the movement and occlusal friction between the particles under cyclic loading. For the selection of cohesion c and internal friction angle φ, the stress-strain curve needs to be used to select the appropriate stress difference $(\sigma_1-\sigma_3)$. In the static test, the stress-strain curve should be observed first. If the stress-strain curve has the largest peak, the stress difference at the peak point should be selected to be the reference basis; if the stress-strain curve has no peak point, then select the corresponding stress difference when the axial strain value is 15% as the reference basis. For the dynamic test, when the strain reaches 5% (Seed *et al*. 2002), it can be selected as the basis for the failure of the soil, and draw different Mohr's stress circles according to the different confining pressures, as shown in Fig. 9. The Mohr's stress circles are $(\sigma_1-\sigma_3)/2$ is the radius, and $(\sigma_1+\sigma_3)/2$ is the abscissa, and then the average straight line (strength envelope) is drawn through the fixed points of each circle. The intercept between the strength envelope and the vertical axis is the dynamic cohesion c, and the inclination angle of the strength envelope is the dynamic internal friction angle φ. Then, the dynamic cohesion c and the dynamic internal friction angle φ are obtained.

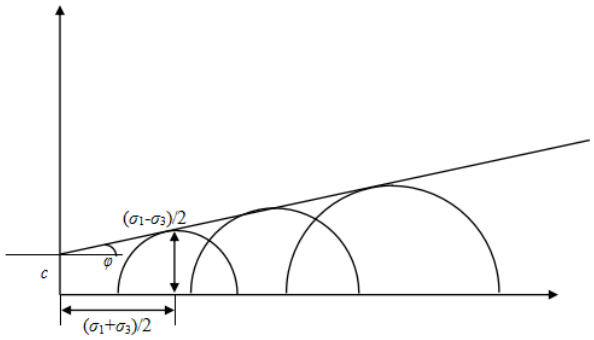

Fig. 9 Mohr's stress circle

4. Results and discussion

In the research of soil dynamic properties, there are many types of dynamic constitutive models of soil, including elastic-plastic models, bilinear models, Martin-Finn-Seed models, and Hardin Drnevich equivalent viscoelastic linear models. Currently, the most widely used model is the Hardin Drnevich equivalent viscoelastic linear model (Hardin *et al.* 1972). For clay, the dynamic constitutive relationship conforms to the Hardin Drnevich equivalent viscoelastic linear model, and the model mainly adopts two parameters, which are equivalent dynamic elastic modulus (or equivalent dynamic shear modulus) and equivalent damping ratio, to reflect the nonlinearity and hysteresis of the dynamic stress-strain relationship of soil.

4.1 Dynamic stress-strain curve

By doing the dynamic triaxial test, the hysteresis loop of clay under cyclic loading is obtained. Taking the maximum dynamic stress and the corresponding strain of the hysteresis loop in each level, the dynamic stress-strain curve of clay can be drawn in Fig. 10, which shows the changing trend of clay under various confining pressures at normal temperatures and different freezing temperatures.

Fig. 10 shows that the dynamic stress has a significant increase in the initial stage of the strain, and gradually becomes flat when increasing the strain. The reason is that the soil in the early stage has a certain integrity of its structure, and thus has a certain ability to resist external dynamic stress, which results in a significant increase in the stress at the early stage of strain. When the confining pressure is applied to the soil, this ability to resist external dynamic stress will be strengthened. For frozen soil, the low temperature makes the water in the soil freeze and transform from liquid to solid, which further improves the ability of the soil to resist external dynamic stress. When

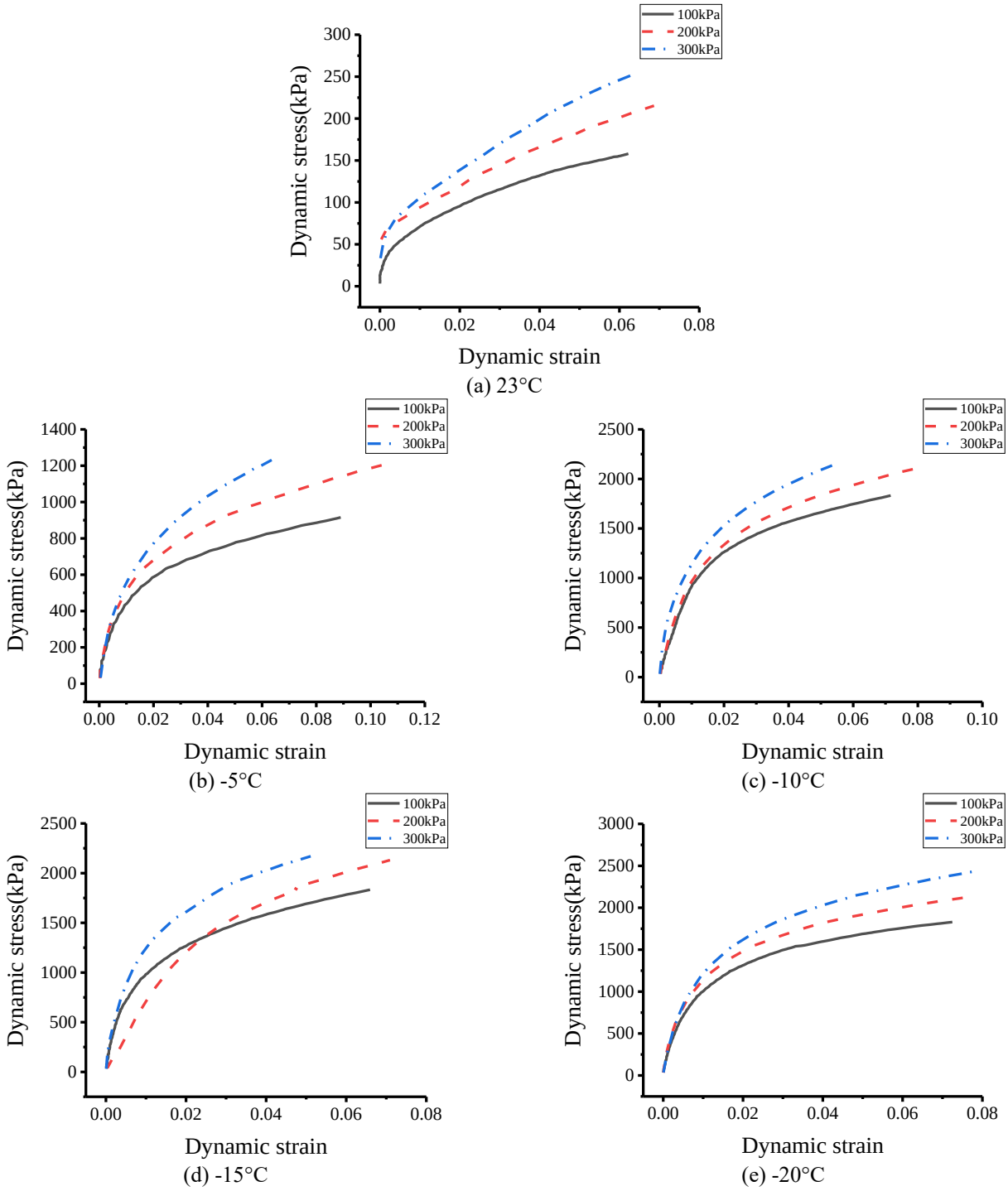

Fig. 10 Dynamic stress-strain curves at different temperatures

the dynamic stress gradually gets a specific critical value, the ability of the soil to resist the external dynamic stress will gradually decrease, resulting in a significant increase in dynamic strain and a slowdown in the trend of dynamic stress increase.

When confining pressure increases and freezing temperature decreases, the slowing down stage of the dynamic stress-strain curve will be delayed. Compared with the situation of the normal temperature soil, the situation of the frozen soil is more significant. This is because the higher the confining pressure, the better the integrity and stability of the soil would be, and the less likely to be damaged. When the soil is frozen, the integrity and stability of the soil will be increased. The lower the freezing temperature, the more obviously the increasing trend is. As a result, the slowdown phase of the dynamic stress-strain curve is delayed.

Regarding the dynamic constitutive relationship of clay, Hardin et al. found a hyperbolic relationship in accordance with Eq. (3) under cyclic loading through a large number of

Table 2 Fitting results

Temperature (°C)	Confining pressure (kPa)	*a*	*b*	R^2
23	100	1.020E-05	0.023	0.949
	200	5.172E-06	0.011	0.823
	300	3.353E-06	0.015	0.901
-5	100	4.075E-06	0.004	0.991
	200	3.619E-06	0.004	0.987
	300	2.937E-06	0.005	0.99
-10	100	2.158E-06	0.003	0.977
	200	2.055E-06	0.003	0.997
	300	1.828E-06	0.001	0.986
-15	100	1.838E-06	0.002	0.986
	200	1.800E-06	0.004	0.993
	300	1.799E-06	0.001	0.993
-20	100	1.747E-06	0.002	0.994
	200	1.729E-06	0.001	0.992
	300	1.717E-06	0.001	0.993

experiments. Eq. (6) can be derived from Eq. (3), Eq. (4), Eq. (5).

$$\sigma_d = \frac{\varepsilon_d}{a + b\varepsilon_d} \tag{3}$$

$$E_d = \frac{\sigma_d - \sigma_0}{\varepsilon_d - \varepsilon_0} = \frac{\sigma_d - 0}{\varepsilon_d - 0} = \frac{\sigma_d}{\varepsilon_d} = \frac{1}{a + b\varepsilon_d} \tag{4}$$

$$E_{d\max} = \lim_{\varepsilon_d \to 0} E_d = \lim_{\varepsilon_d \to 0} \frac{1}{a + b\varepsilon_d} = \frac{1}{a} \tag{5}$$

$$\sigma_{d\max} = \lim_{\varepsilon_d \to \infty} \sigma_d = \lim_{\varepsilon_d \to \infty} \frac{1}{a + b\varepsilon_d} = \frac{1}{b} \tag{6}$$

where σ_d is the dynamic stress, ε_d is the dynamic strain, *a* and *b* are the soil parameter respectively.

In order to verify that the dynamic stress-strain curve of the clay used in this experiment conforms to the Hardin Drnevich hyperbolic model, the SPSS software is used to fit its dynamic stress-strain curve to the Hardin Drnevich hyperbolic model, and the fitting results are ideal. The results are presented in Table 2.

Table 2 shows that the variances are all close to 1, indicating that the fitting results are very ideal. Especially for frozen soil, the fitting result is better than that of normal temperature. The reason is the frozen soil is with higher strength. The cyclic stress exerted by the loading hammer during the test loading process is more stable. The strength of frozen soil will be significantly reduced, resulting in small fluctuations in the applied cyclic stress. Such fluctuations will lead to relatively poor fitting results for normal temperature soils.

4.2 Dynamic elastic modulus

The dynamic elastic modulus represents the ability of soil to resist deformation. It is a physical quantity that describes the elasticity of materials. It is a general term. From a microscopic point of view, it reflects the bonding strength between molecules, atoms, or ions. Under the action of cyclic stress and the same confining pressure, the dynamic elastic modulus of clay will gradually decrease when increasing dynamic strain, as shown in Fig. 11.

Table 3 Growth rate of dynamic elastic modulus at negative temperature compared to positive temperature (%)

Confining pressure (kPa) \ Temperature(°C)	-5	-10	-15	-20
100	152.3	375.8	456.2	458.9
200	42.2	151.0	188.2	199.2
300	12.9	81.7	86.5	95.0

The reason is that when increasing the strain, the integrity and stability of the soil gradually decrease, the density of the soil will continue to decrease, and the distance between the particles will gradually increase. In this circumstance, the cementation force between the soil particles will be weakened, and the original structure will be affected, weakening the ability of the soil to resist deformation, which decreases the dynamic elastic modulus.

Fig. 12 presents the change of dynamic elastic modulus with different temperatures. Under the same confining pressure, the dynamic elastic modulus of clay at normal temperature is significantly lower than at frozen temperature. The results of this experiment show a similar trend to previous studies (e.g., Czajkowski *et al.* 1980, Christ *et al.* 2009, Xu *et al.* 2020).

The percentage increase in the dynamic elastic modulus of clay under various negative temperatures, compared to positive temperature conditions at confining pressures of 100 kPa, 200 kPa, and 300 kPa, is shown in Table 3.

As seen in Fig. 12, the dynamic elastic modulus of clay is at its lowest in summer. With the change of seasons to autumn, the temperature decreases. The clay is frozen, its dynamic elastic modulus will increase sharply. When the freezing temperature decreases from -5°C to -10°C, the dynamic elastic modulus increases more dramatically. When the freezing temperature reaches -15°C, the upward trend will gradually weaken. As winter approaches and the temperature continues to decrease to -20°C, there is a gradual increase in the dynamic elastic modulus. In addition, the content depicted in the figure does not imply that the results between different temperatures represent a linear relationship. However, in order to better observe its changes, a method of straight line connection has been adopted, including the temperature comparisons presented below.

This phenomenon is attributed to the gradual decrease in temperature from summer to winter. When the temperature drops below freezing, the water in the clay freezes, forming many ice crystals. The lower the temperature of the clay, the more ice crystals form within it. The existence of ice crystals enhances the cementation force between clay particles, resulting in strong stiffness of frozen clay and a

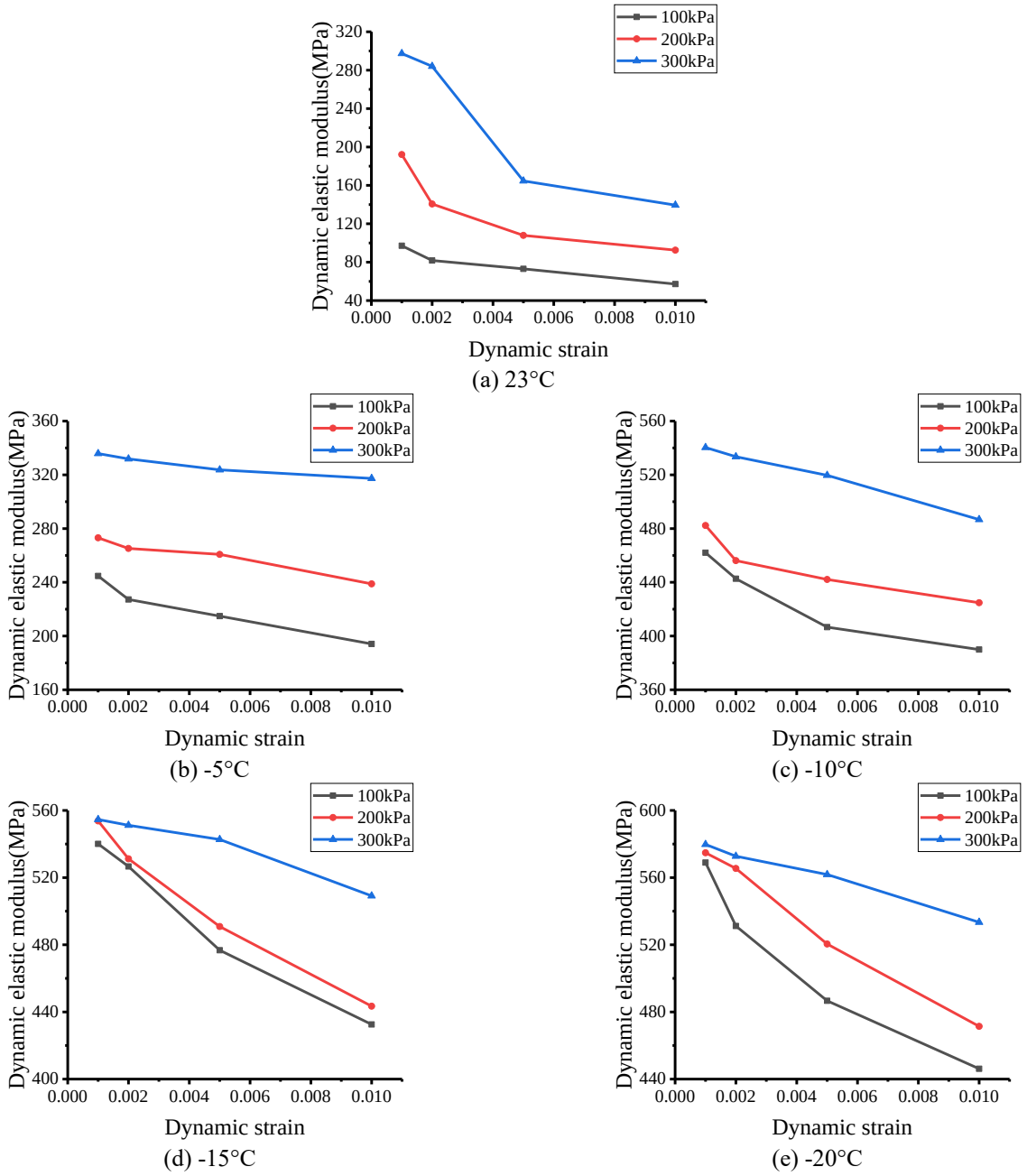

Fig. 11 Dynamic elastic modulus-strain curves at different temperatures

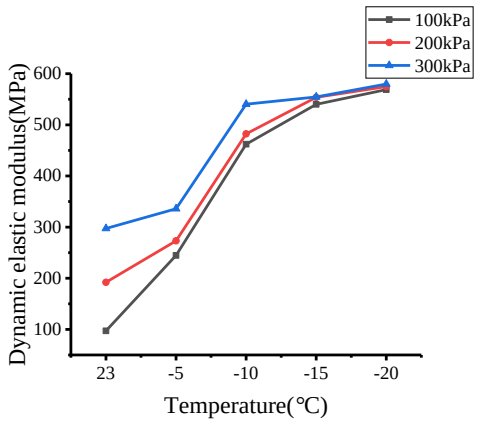

Fig. 12 Dynamic elastic modulus-temperature curves under different confining pressures

modulus tends to increase more gently. Observing Fig. 12, as the season transitions from late autumn to winter, specifically when the environmental temperature is at -15°C and -20°C, the freezing temperature of clay is quite low, and the confining pressure exerts a minimal effect on the dynamic elastic modulus of clay under initial strain. This is attributed to the significantly low temperatures in winter, which enhance the internal structural strength and stiffness of the clay. At this juncture, the presence of confining pressure has a comparatively weaker impact on its strength than in the case of soil at normal temperatures.

From this analysis, it can be inferred that the dynamic elastic modulus of clay is at its lowest during summer due to higher ambient temperatures and the absence of ice crystals within the clay. At the end of spring and the

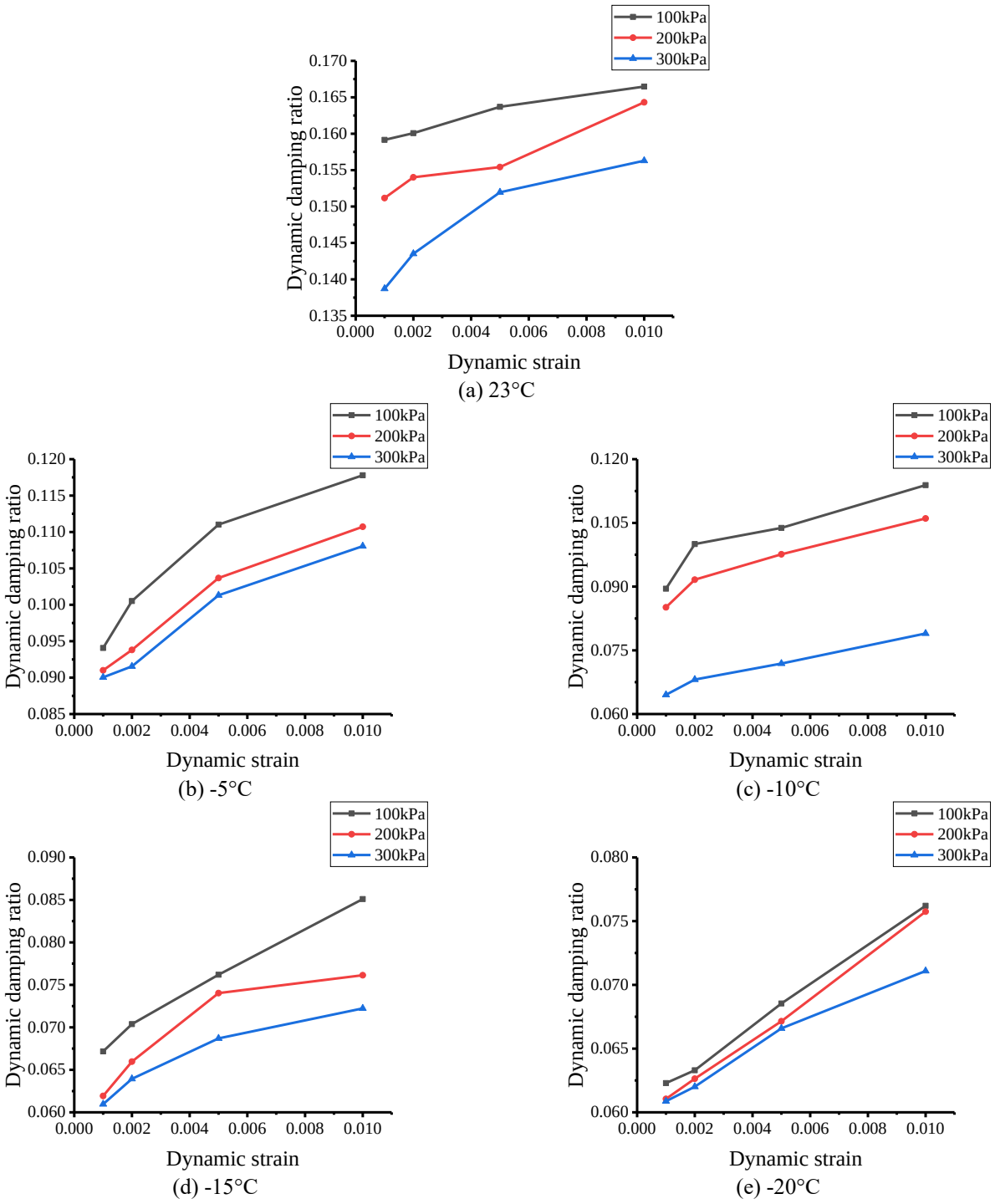

Fig. 13 Dynamic damping ratio-strain curves at different temperatures

beginning of autumn, when temperatures drop noticeably, the emergence of ice crystals causes significant changes in the internal structure of the soil, leading to a noticeable increase. In the early spring and late autumn, as temperatures continue to decrease, the significant increase in ice crystals results in an even more pronounced increase. During winter, the dynamic elastic modulus reaches its maximum value.

Fig. 12 shows that when the clay freezes, the confining pressure will have a great impact on it. With the confining pressure of 100 kPa, the dynamic elastic modulus will be greatly improved. When increasing the confining pressure to 200 kPa, the increasing trend will slow down, and when the confining pressure reaches 300 kPa, the trend will become gentler. When the temperature keeps decreasing, the confining pressure has little effect on the variation trend of the dynamic elastic modulus. The existence of confining pressure will close the cracks between the clay, and the compactness of the clay will increase, thus, its strength and stiffness will increase. The greater the confining pressure,

the greater the pressure on the clay sample, and thus the dynamic elasticity of the clay would be. The modulus will increase as the confining pressure increases. For frozen soil, with the confining pressure of 100 kPa, the confining pressure exerts a squeezing effect on the clay sample. In this circumstance, the temperature decreases and the clay freezes. The cracks between the clay will be connected by ice crystals, and the dynamic elastic modulus will improve significantly. With the confining pressure going up to 200 kPa, the confining pressure has a stronger squeezing effect on the normal temperature clay and frozen clay, leading to a significant increase in its initial dynamic elastic modulus. However, because of the enhancement of the extrusion effect, the increase of the dynamic elastic modulus of clay during freezing slows down. When the confining pressure continues to increase to 300 kPa, the increasing trend of dynamic elastic modulus will continue to weaken. As a whole, the dynamic elastic modulus of clay will increase as confining pressure increases, no matter whether it is at the same temperature or at the same strain.

4.3 Dynamic damping ratio

Under dynamic load, the soil body vibrates to produce a certain amount of energy. At the same time, it produces a certain amount of damping to the shock wave, and the dynamic damping ratio is an important parameter that reflects the amount of energy produced by the soil body absorbing vibration. Fig. 13 shows that the dynamic damping ratio of clay will gradually increase as the strain increases.

The reason is that the increase of strain weakens the bond between clay particles and ice crystals. When the strain reaches a certain degree, the connection will be destroyed, the clay sample will produce new cracks, and the hysteretic energy consumption will increase, leading to the increased of dynamic damping ratio.

When the soil is frozen, the dynamic damping ratio will decrease sharply. The results of this experiment show a similar trend to previous studies (e.g., Czajkowski *et al.* 1980, Wu *et al.* 2019, Liu *et al.* 2020). When decreasing the freezing temperature, the dynamic damping ratio will continue to decrease, but the downward trend will gradually slow down, as shown in Fig. 14.

The percentage decrease in the dynamic damping ratio of clay under various negative temperatures, compared to positive temperature conditions at confining pressures of 100 kPa, 20 0kPa, and 300 kPa, is shown in Table 4.

This phenomenon occurs because the transition from summer to autumn, with the accompanying temperature decrease, causes the water in the clay to freeze, leading to a reduction in the content of unfrozen water. The frozen water transforms into solid ice crystals, which enhance the cementation forces within the clay, thereby weakening its ability to absorb dynamic energy and consequently reducing the dynamic damping ratio. As winter sets in and the environmental temperature drops significantly, the content of unfrozen water in the clay becomes negligible, while the content of ice crystals reaches a level beyond which it does not increase further, slowing down the declining trend of

Table 4 Attenuation rate of dynamic damping ratio at negative temperature compared to positive temperature (%)

Confining pressure (kPa) \ Temperature(°C)	-5	-10	-15	-20
100	40.9	43.8	57.8	60.9
200	39.8	43.7	59.1	59.6
300	35.1	53.5	56.1	56.1

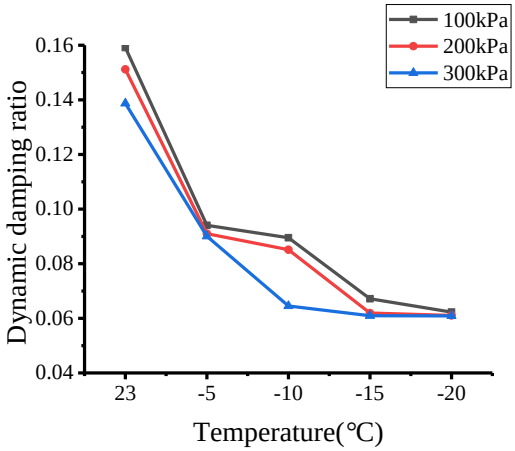

Fig. 14 Dynamic damping ratio-temperature curves under different confining pressures

the clay's dynamic damping ratio. The reverse can be inferred as the season transitions from winter to summer. Overall, under the same temperature or strain, the dynamic damping ratio of clay gradually decreases with increasing confining pressure. This is because an increase in confining pressure reduces the clay's ability to absorb dynamic energy, leading to such an outcome.

Hence, it can be deduced that in summer, due to higher temperatures, the cementation forces between particles within the clay are weaker, and its capacity to absorb dynamic energy is stronger, resulting in a higher dynamic damping ratio. At the end of spring and the beginning of autumn, the reduction in temperature weakens this energy absorption capacity, leading to a noticeable decrease. In the early spring and late autumn, the decreasing trend slows down. During winter, the dynamic damping ratio reaches its minimum value.

4.4 Dynamic cohesion

The dynamic cohesion c reflects the various physical and chemical forces generated between soil particles under dynamic loads, including Van der Waals force, cementation force, and Coulomb force. The dynamic cohesion is obtained from the Mohr's stress circle. Fig. 15 shows the Mohr's stress circle of normal temperature clay and frozen clay respectively. The Mohr's stress circle of the two working conditions has a certain difference. It can be seen that the distance between the three Mohr's stress circles under the three different confining pressures of the normal temperature clay is relatively far, and for the frozen clay, the distance between the three Mohr's stress circles under the

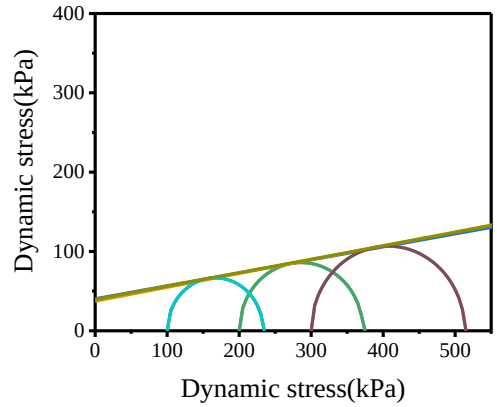

(a) 23℃

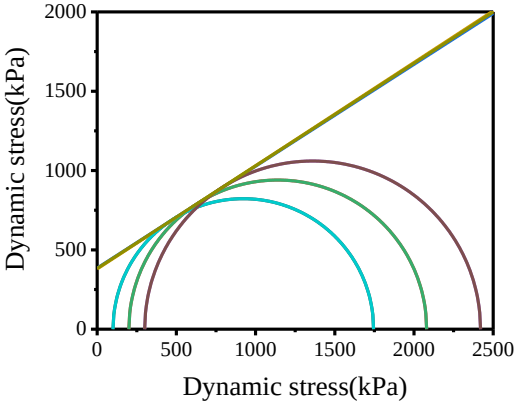

(b) -20℃

Fig. 15 Comparison of different Mohr's stress circles

three different confining pressures is very close. Since the normal-temperature clay produces a modest force to produce strain, whereas the frozen clay exerts a considerable force, the results in Fig. 15 are significantly different.

Fig. 16 shows the variation of dynamic cohesion c with temperature. After the clay is frozen, the dynamic cohesion will increase significantly. The results of this experiment show a similar trend to previous studies (e.g., Czurda *et al.* 1997, Oh *et al*. 2011, Al-Hunaidi *et al.* 2011). When the freezing temperature decreases continuously, the increasing trend gradually decreases. At the freezing temperature of -10°C, the dynamic cohesion will no longer increase significantly. The dynamic cohesion of clay at -5°C is 346.13% higher than that at normal temperature. The dynamic cohesion of clay at -10°C is 783.8% higher than that at normal temperature. The dynamic cohesion of clay at -15°C is 844.84% higher than that at normal temperature. The dynamic cohesion of clay at -20°C increased by 883.31% compared with that at normal temperature.

This is due to the transition from summer to autumn, where the temperature drops and the soil undergoes freezing. The water content in clay transforms into ice crystals, strengthening the cementation between clay particles. At this point, the clay particles and ice crystals collectively bear the shear strength of the clay, leading to an

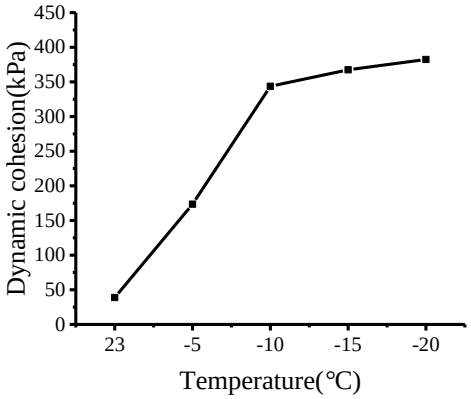

Fig. 16 Dynamic cohesion-temperature curve

increase in dynamic cohesion. In autumn, at the onset of soil freezing, the unfrozen water in the clay gradually turns into ice crystals, continuously enhancing the cementation force and significantly increasing the dynamic cohesion. In winter, the content of unfrozen water in the soil is minimal, resulting in a slow increase in ice crystals, and thus, the trend of increasing dynamic cohesion slows down.

From this analysis, it can be deduced that in summer, due to higher temperatures and the absence of ice crystals, clay exhibits lower shear strength, leading to minimal dynamic cohesion. At the end of spring and the beginning of autumn, with the decrease in environmental temperature and the appearance of ice crystals, there is a notable increase in dynamic cohesion. In early spring and late autumn, as the temperature continues to decrease and the amount of ice crystals increases, the increase in dynamic cohesion remains significant. In winter, this increasing trend slows down, and dynamic cohesion reaches its maximum value.

4.5 Dynamic internal friction angle

The dynamic internal friction angle φ mainly represents the movement and occlusal friction between particles under the dynamic load.

Fig. 17 shows that when the soil is frozen, the dynamic internal friction angle will increase significantly. The results of this experiment show a similar trend to previous studies (e.g., Czurda *et al.* 1997, Jiang *et al.* 2017, Tong *et al.* 2018). The lower the freezing temperature, the greater the dynamic internal friction angle would be. The dynamic internal friction angle at -5°C is 185.19% higher than that at normal temperature. The dynamic internal friction angle at -10°C is 255.47% higher than that at normal temperature. The dynamic internal friction angle at -15°C is 246.61% higher than that at normal temperature. The dynamic internal friction angle at -20°C increased by 242.86% compared with that at normal temperature.

The contact area between clay particles greatly influences the dynamic internal friction angle of clay, and the arrangement of the clay particles also has a significant impact. As the season transitions from summer to autumn and the temperature decreases, causing the clay to freeze,

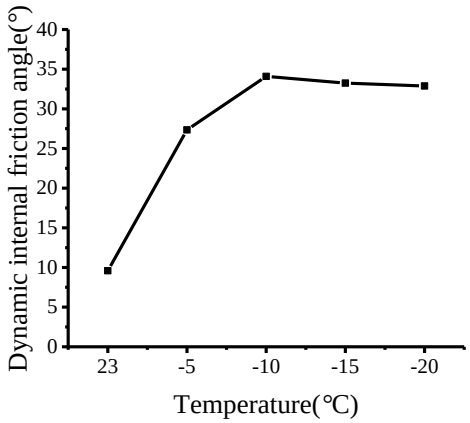

Fig. 17 Dynamic internal friction angle-temperature curve

the resulting frost heave force enlarges the contact area between soil particles, thus increasing the dynamic internal friction angle φ. The lower the environmental temperature, the stronger the frost heave force exerted on the clay particles, and consequently, the larger the dynamic internal friction angle φ. When the temperature reaches -10°C and beyond, as the season transitions from autumn to winter, changes in the dynamic internal friction angle tend to stabilize. This is because once a certain negative temperature is reached, further lowering the environmental temperature does not continuously increase the contact area between clay particles, resulting in no significant change in the dynamic internal friction angle.

Hence, it can be concluded that in summer, due to higher temperatures and the absence of frost heave force, the dynamic internal friction angle of clay is at its lowest.

At the end of spring and the beginning of autumn, as temperatures decrease and frost heave force causes an increase in the contact area between soil particles, there is a noticeable increase in the dynamic internal friction angle. In early spring and late autumn, as temperatures continue to fall, the impact of the frost heave force on the soil compared to the onset of freezing diminishes, so the increasing trend slows down. In winter, the dynamic internal friction angle gradually stabilizes with a slight decrease.

Given that the lowest temperature set for the experiments was -20°C, the experimental results and changes in various parameters showed that when the temperature dropped from -15°C to -20°C, the changes in soil property parameters were minimal. This suggests that when the temperature continues to decrease marginally, there will not be significant changes in the dynamic properties of the soil.

5. Conclusions

In this paper, a dynamic triaxial test was carried out for clay in the Harbin area at 3 confining pressures (100 kPa, 200 kPa, 300 kPa) and 5 different temperatures (23°C, -5°C, -10°C, -15°C, -20°C). Using the temperature variation to reflect the change of seasons. The dynamic stress-strain curve of the clay is obtained, and the dynamic elastic modulus, dynamic damping ratio, dynamic cohesion, and dynamic internal friction angle of the clay are measured and analyzed. And analyze the evolving patterns of its changes with the alternation of seasons. The following conclusions are drawn:

- The dynamic stress increases significantly in the initial stage of strain, and gradually tends to level off as the strain continues to increase. With the increase of the confining pressure and the decrease of the freezing temperature, the slowing down stage of the dynamic stress-dynamic strain curve will be delayed. Compared with the trend of the normal temperature soil, the situation of this trend in the frozen soil is more significant.
- Under the action of cyclic stress and the same confining pressure, the dynamic elastic modulus of clay will gradually decrease with the increase of dynamic strain. The dynamic elastic modulus of clay at normal temperature is significantly lower than the dynamic elastic modulus of clay when frozen. With the continuous decrease of freezing temperature, the increase of dynamic elastic modulus tends to be gentle. When the freezing temperature is between -15°C and -20°C, which means, when the freezing temperature is very low, the confining pressure has little effect on the dynamic elastic modulus of the clay under the initial strain.
- The dynamic damping ratio of clay will gradually increase when increasing the strain. When the soil is frozen, the dynamic damping ratio will decrease significantly. When the freezing temperature decreases, the dynamic damping ratio will continue to decrease, but the downward trend will gradually slow down.
- After freezing, both the dynamic cohesion and dynamic internal friction angle of clay increase significantly. Once the temperature reaches -10°C, this increasing trend slows down and tends to stabilize.
- By analyzing the evolutionary patterns of dynamic characteristics of clay in the sequence of seasonal changes in spring, summer, autumn, and winter, it is observed that the dynamic elastic modulus, dynamic cohesion, and dynamic internal friction angle exhibit a decreasing trend followed by an increasing trend, whereas the dynamic damping ratio demonstrates an increasing trend followed by a decreasing trend.

Acknowledgments

This work was supported by the National Key Research and Development Program of China [2018YFD1100405]; Scientific Research Fund of Institute of Engineering Mechanics, China Earthquake Administration [2018D19].

References

Abuel-Naga, H.M., Bergado, D.T., Bouazza, A. and Pender, M.J. (2009), "Thermal conductivity of soft Bangkok clay from laboratory and field measurements", *Eng. Geol.,* **105**(3-4), 211-219. https://doi.org/10.1016/j.enggeo.2009.02.008.

Aldaood, A., Bouasker, M. and Al-Mukhtar, M. (2016), "Effect of water during freeze–thaw cycles on the performance and

durability of lime-treated gypseous soil", *Cold Reg. Sci. Technol.*, **123**, 155-163. https://doi.org/10.1016/j.coldregions.2015.12.008.

Al-Hunaidi, M.O., Chen, P.A., Rainer, J.H. and Tremblay, M. (2011), "Shear moduli and damping in frozen and unfrozen clay by resonant column tests", *Can. Geotech. J.*, **33**(3), 510-514. https://doi.org/10.1139/t96-073.

Bo, Y.F., Chen, G.X., Zhou, Z.L. and Wu, Q. (2021), "Comparison research on the normalized dynamic shear modulus and damping ratio by resonant column and cyclic triaxial tests", *J. Disaster Prevent. Mitigation Eng.*, **41**(2), 343-349. https://doi.org/10.13409/j.cnki.jdpme.20191017003.

Cheng, S., Wang, Q., Fu, H.C., Wang, J.Q., Han, Y., Shen, J.J. and Lin, S. (2021), "Effect of freeze-thaw cycles on the mechanical properties and constitutive model of saline soil", *Geomech. Eng.*, **27**(4), 309-322. https://doi.org/10.12989/gae.2021.27.4.309.

Chen, S.J., Ma, W., Li, G.Y., Liu, E.L. and Zhang, G. (2017), "Development and application of triaxial apparatus of frozen soil used in conjunction with medical CT", *Rock Soil Mech.*, **38**(2), 359-367. https://doi.org/10.16285/j.rsm.2017.S2.049.

Christ, M., Kim, Y.C. and Park, J.B. (2009), "The Influence of temperature and cycles on acoustic and mechanical properties of frozen soils", *KSCE J. Civil Eng.*, **13**(3), 153-159. https://doi.org/10.1007/s12205-009-0153-1.

Czajkowski, R.L. and Vinson, T.S. (1980), "Dynamic properties of frozen silt under cyclic loading", *J. Geotech. Geotech. Eng. Division*, **106**(9), 963-980. https://doi.org/10.1016/0022-1694(80)90029-3.

Czurda, K.A. and Hohmann, M. (1997), "Freezing effect on shear strength of clayey soils", *Appl. Clay Sci.*, **12**(1-2), 165-187. https://doi.org/10.1016/s0169-1317(97)00005-7.

Esmaeili-Falak, M., Katebi, H. and Javadi, A.A. (2020), "Effect of freezing on stress–strain characteristics of granular and cohesive soils", *J. Cold Reg. Eng.*, **34**(2), 05020001. https://doi.org/10.1061/(ASCE)CR.1943-5495.0000205.

Esmaeili-Falak, M., Katebi, H., Vadiati, M. and Adamowski, J. (2019), "Predicting triaxial compressive strength and young's modulus of frozen sand using artificial intelligence methods", *J. Cold Reg. Eng.*, **33**(3), 04019007. https://doi.org/10.1061/(ASCE)CR.1943-5495.0000188.

Fard, A.R., Moradi, G., Ghalehjough, B.K. and Abbasnejad, A. (2020), "Freezing-thawing resistance evaluation of sandy soil, improved by polyvinyl acetate and ethylene glycol monobutyl ether mixture", *Geomech. Eng.*, **23**(2), 179-187. https://doi.org/10.12989/gae.2020.23.2.179.

Fredlund, D.G. (2006), "Unsaturated soil mechanics in engineering practice", *J. Geotech. Geoenviron. Eng.*, **132**(3), 286-321. https://doi.org/10.1061/(ASCE)1090-0241(2006)132:3(286).

Garakani, A.A., Haeri, S.M., Khosravi, A. and Habibagahi, G. (2015), "Hydro-mechanical behavior of undisturbed collapsible loessial soils under different stress state conditions", *Eng. Geol.*, **195**, 28-41. https://doi.org/10.1016/j.enggeo.2015.05.026.

Girgis, N. (2019), "Experimental investigations on temperature-dependent mechanical properties of artificially frozen sandy clay soils", Montreal: Concordia University.

Girgis, N., Li, B., Akhtar, S. and Courcelles, B. (2020), "Experimental study of rate-dependent uniaxial compressive behaviors of two artificial frozen sandy clay soils", *Cold Reg. Sci. Technol.*, **180**, 103166. https://doi.org/10.1016/j.coldregions.2020.103166.

Güler, E. and Afacan, K.B. (2021), "Dynamic behavior of clayey sand over a wide range using dynamic triaxial and resonant column tests", *Geomech. Eng.*, **24**(2), 105-113. https://doi.org/10.12989/gae.2021.24.2.105.

Hardin, B.O. and Drnevich, V.P. (1972), "Shear modulus and damping in soils: measurement and parameter effects", *ASCE Soil Mech. Found. Division J.*, **98**(6), 603-624. https://doi.org/10.1061/JSFEAQ.0001756.

Ishihara, K., Yoshida, N. and Tsujino, S. (1985), "Modelling of stress-strain relations of soils in cyclic loading", *Proceedings of the International Conference on Numerical Methods in Geomechanics*.

Jiang, W.Y., Yang, P., Chen, B. and He, W.L. (2017), "Experimental study on strength properties of artificial frozen soil in marine soft soil area of Ningbo city, China", *J. Forestry Eng.*, **2**(5), 126-131. https://doi.org/10.13360/j.issn.2096-1359.2017.05.022.

Kallioglou, P., Tika, T. and Pitilakis, K. (2008), "Shear modulus and damping ratio of cohesive soils", *J. Earthq. Eng.*, **12**(6), 879-913. https://doi.org/10.1080/13632460802536552.

Kang, X., Ge, L., Chang, K.T. and Kwok, A.O. (2015), "Strain-Controlled Cyclic Simple Shear Tests on Sand with Radial Strain Measurements", *J. Mater. Civil Eng.*, 04015169. https://doi.org/10.1061/(ASCE)MT.1943-5533.0001458.

Kang, X., Ge, L. and Cheng, Y. (2015), "Radial strain behaviors and stress state interpretation of soil under direct simple shear", *J. Test. Eval.*, **43**(6), 1-8.

Kim, S.Y., Kim, Y. and Lee, J.S. (2021), "Effects of frozen water content and silt fraction on unconfined compressive behavior of fill materials", *Constr. Build. Mater.*, **266**, 120912. https://doi.org/10.1016/j.conbuildmat.2020.120912.

Kumar, A. and Soni, D.K. (2020), "Strength and microstructural characterisation of plastic soil under freeze and thaw cycles", *Indian Geotech. J.*, **50**, 359-371. https://doi.org/10.1007/s40098-019-00372-8.

Lee, J.S., Yu, J.D., Han, K. and Kim, S.Y. (2020), "Strength characteristics of sand-silt mixtures subjected to cyclic freezing-thawing-repetitive loading", *Sensors*, **20**(18), 5381. https://doi.org/10.3390/s20185381.

Le, K.N. and Ghayoomi, M. (2017), "Cyclic direct simple shear test to measure strain-dependent dynamic properties of unsaturated sand", *Geotech. Test. J.*, **40**(3), 381-395. https://doi.org/10.1520/GTJ20160128.

Li, M.M., Niu, Y.H., Jiang, C., Mu, Q.S. and Li, Z.P. (2016), "Recent progress of excavation and breaking methods for frozen soil", *Mech. Eng.*, **38**(2), 126-133. https://doi.org/10.6052/1000-0879-15-049.

Liu, J.K., Cui, Y.H., Liu, X. and Chang, D. (2020), "Dynamic characteristics of warm frozen soil under direct shear test-comparison with dynamic triaxial test", *Soil Dyn. Earthq. Eng.*, **133**, 106114. https://doi.org/10.1016/j.soildyn.2020.106114.

Li, X.L., Wang, H.J., Zou, S.J., Ma, H.C. and Niu, Y.H. (2017), "Research state of deformation characteristics of frozen soil under cyclic loading and problems in frozen soil excavation", *J. Glaciology and Geocryology*, **39**(1), 92-101. https://doi.org/10.7522/j.issn.1000-0240.2017.0012.

Ma, W. and Su, Y.Q. (2021), "Advances on seismic safety study of the permafrost sites along Qinghai-Tibet project corridor", *J. Disaster Prevent. Mitigation Eng.*, **41**(4), 723-733. https://doi.org/10.13409/j.cnki.jdpme.2021.04.003.

Mosallamy, M.E., Fattah, T. and Khouly, M.E. (2016), "Experimental study on the determination of small strain-shear modulus of loess soil", *HBRC J.*, **12**(2), 181-190. https://doi.org/10.1016/j.hbrcj.2014.11.010.

Mu, R., Huang, Z.H., Pu, S.Y., Yao, Z.H. and Cheng, X. (2020), "Accumulated deformation characteristics of undisturbed red clay under cyclic loading and dynamic constitutive relationship", *Rock Soil Mech.*, **42**(2), 1-10. https://doi.org/10.16285/j.rsm.2020.0719.

Oh, M.Y., Bang, K.H., Hong, S.S., Kim, Y.S. and Cho, W.J. (2011), "Freezing effects on strength characteristics of Antarctic ground under Jang Bogo station", *Proceedings of the Korean*

Geo-Environmental Society.

Okamura, M. and Tamamura, S. (2011), "Seismic stability of embankment on soft soil deposit", *Int. J. Phys. Model. Geotech.*, **11**(2), 50-57. https://doi.org/10.1680/ijpmg.2011.11.2.50.

Onur, M.I., Tuncan, M. and Tuncan, A. (2014), "An experimental study for determining the shear modulus of Toyoura sand", *Proceedings of the 2nd European Conference on Earthquake Engineering and Seismology*, Istanbul.

Reznik, Y.M. (2007), "Influence of physical properties on deformation characteristics of collapsible soils", *Eng. Geol.*, **92**(1-2), 27-37. https://doi.org/10.1016/j.enggeo.2007.03.001.

Seed, H.B. and Lee, K.L. (2002), "Liquefaction of saturated sand during cyclic loading", *Geotechnical Special Publication*, **92**(118), 105-134. https://doi.org/10.1061/JSFEAQ.0000913.

Shelman, A., Tantalla, J., Sritharan, S. and Nikolaou, S. (2014), "Characterization of seasonally frozen soils for seismic design of foundations", *J. Geotech. Geoenviron. Eng.*, **140**(7), 1-10. https://doi.org/10.1061/(ASCE)GT.1943-5606.0001065.

Shogaki, T., Nochikawa, Y. and Sakamoto, T. (2003), "Consolidation properties of Pusan new port clays", *Pusan Korea: Proceedings of the Korea-Japan Joint Workshop*.

Tamotsu, M., Kazuhiro, O. and Koji, Y. (2004), "Geotechnical information and engineering practice for constructing man-made island in Osaka Bay", *Engineering Practice and Performance of Soft Deposits, IS-OSAKA*, 561-586.

Teachavorasinskun, S. Thongchim, P. and Lukkunaprasit, P. (2002), "Shear modulus and damping of soft Bangkok clays", *Can. Geotech. J.,* **39**(5), 1201-1208. https://doi.org/10.1139/t02-048.

Thomas, H.R. and Rees, S.W. (2010), "The numerical simulation of seasonal soil drying in an unsaturated clay soil", *Int. J. Numer. Anal. Method. Geomech.*, **17**(2), 119-132. https://doi.org/10.1002/nag.1610170204.

Tong, S.J., Deng, Y.B., Chen, F., Liu, G.B. and Bao, X.M. (2018), "Study on settlement characteristics of energy piles considering temperature effect", *Build. Struct.*, **48**(21), 119-123. https://doi.org/10.19701/j.jzjg.2018.21.023.

Tounsi, H., Rouabhi, A., Jahangir, E. and Guérin, F. (2020), "Mechanical behavior of frozen metapelite: Laboratory investigation and constitutive modeling", *Cold Reg. Sci. Technol.*, **175**, 103058. https://doi.org/10.1016/j.coldregions.2020.103058.

Viran, P.A.G. and Binal, A. (2018), "Effects of repeated freeze-thaw cycles on physico-mechanical properties of cohesive soils", *Arabian J. Geosci.*, **11**(11), 1-13. https://doi.org/10.1007/s12517-018-3592-5.

Voottipruex, P. and Jamsawang, P. (2014), "Characteristics of expansive soils improved with cement and fly ash in Northern Thailand", *Geomech. Eng.*, **6**(5), 437-453. https://doi.org/10.12989/gae.2014.6.5.437.

Wang, Q., Li, N., Wang, P., Hou, P.B., Zhong, X.M., Wang, J. and Wang, H.J. (2017), "Behaviors of dynamic modulus and damping ratio of loess in Gannan region of Gansu Province", *Chinese J. Geotech. Eng.*, **39**(1), 192-197. https://doi.org/10.11779/CJGE2017S1038.

Wijeweera, H. and Joshi, R.C. (1990), "Compressive strength behavior of fine-grained frozen soils", *Can. Geotech. J.*, **27**(4), 472-483. https://doi.org/10.1139/t90-062.

Wijeweera, H. and Joshi, R.C. (1991), "Creep behavior of fine-grained frozen soils", *Can. Geotech. J.*, **28**(4), 489-502. https://doi.org/10.1139/t91-066.

Wijeweera, H. and Joshi, R.C. (2011), "Creep behavior of fine-grained frozen soils: Reply", *Can. Geotech. J.*, **28**(4), 489-502. https://doi.org/10.1139/t93-034.

Wu, Z.J., Zhang, D., Zhao, T., Ma, J.L. and Zhao, D.Y. (2019), "An experimental research on damping ratio and dynamic shear modulus ratio of frozen silty clay of the qinghai-tibet engineering corridor", *Transport. Geotech.*, **21**, 100269. https://doi.org/10.1016/j.trgeo.2019.100269.

Xie, D.Y. (2011), "Soil dynamics", *Beijing: Higher Education Press*.

Xu, X.T., Wang, B.X., Fan, C.X. and Zhang, W.D. (2020), "Strength and deformation characteristics of silty clay under frozen and unfrozen states", *Cold Reg. Sci. Technol.*, **172**, 102982. https://doi.org/10.1016/j.coldregions.2019.102982.

Yamamoto, Y. and Springman, S.M. (2014), "Axial compression stress path tests on artificial frozen soil samples in a triaxial device at temperatures just below 0°C", *Can. Geotech. J.*, **51**(10), 1178-1195. https://doi.org/10.1139/cgj-2013-0257.

Yang, A.W., Zhong, T., Zhang, G.J. and Zhao, M.S. (2018), "Experimental study on dynamic behavior of structural soft clay under cyclic loading", *Earthq. Eng. Eng. Vib.*, **38**(1), 44-50. https://doi.org/ 10.13197/j.eeev.2018.01.44.yangaw.006.

Yasuhara, K., Murakami, S., Song, B.W., Yokokawa, S., Adrian, F.L. and Hyde. (2003), "Postcyclic degradation of strength and stiffness for low plasticity silt", *J. Geotech. Geoenviron. Eng.*, **129**(8), 756-769. https://doi.org/10.1061/(ASCE)1090-0241(2003)129:8(756).

Zhang, J.M. (2012), "New advances in basic theories of sand dynamics", *Chinese J. Geotech. Eng.*, **34**(1), 1-50. https://doi.org/CNKI:SUN:YTGC.0.2012-01-000.

Zheng, X.Q., Fan, G.S. and Xing, S.Y. (2002), "Movement of the moisture content in seasonal non-saturated freezing and thawing soil", *Beijing: Geology Press*.

GC